

Fluorescent Peptides Labeled with Environment-Sensitive 7-Aminocoumarins and Their Interactions with Lipid Bilayer Membranes and Living Cells

Tokiko Murase, Toshitada Yoshihara, Keiichi Yamada, and Seiji Tobita*

Department of Chemistry and Chemical Biology, Gunma University, Kiryu, Gunma 376-8515

Received November 13, 2012; E-mail: tobita@gunma-u.ac.jp

The photophysical properties of protected nonnatural amino acids Boc-L-Dap(7DEAC)-OMe (7DEAC: 7-diethylaminocoumarin) and Boc-L-Dap(C343)-OMe (C343: coumarin 343) were investigated to evaluate the suitability of these amino acids as fluorescent units in peptide-based fluorescent biosensors. The absorption and fluorescence spectra of Boc-L-Dap(7DEAC)-OMe and Boc-L-Dap(C343)-OMe exhibited significant red shifts with increasing solvent polarity. The fluorescence quantum yield and lifetime of Boc-L-Dap(7DEAC)-OMe solutions decreased remarkably with increasing solvent polarity, whereas those of Boc-L-Dap(C343)-OMe were slightly affected by the solvent polarity. Fluorescent peptides H-Dap(7DEAC)-LLA-OMe (**1**), H-Dap(7DEAC)-KLA-OMe (**2**), and H-Dap(7DEAC)-ELA-OMe (**3**) labeled with environment-sensitive 7DEAC were synthesized to examine the interactions of these labeled peptides with lipid membranes and living cells. Neutral 1,2-dimyristoyl-*sn*-glycero-3-phosphocholine (DMPC) and anionic 1,2-dimyristoyl-*sn*-glycero-3-[phospho-*rac*-(1-glycerol)] (DMPG) liposomes were used to investigate peptide-membrane interactions. Hydrophobic peptide **1** exhibited high affinities to both DMPC and DMPC/DMPG mixed membranes. Of the three peptides, cationic peptide **2** exhibited the strongest affinity to DMPC/DMPG membranes, whereas anionic peptide **3** showed a much lower affinity to DMPC/DMPG membranes. These results could be interpreted based on hydrophobic and electrostatic interactions between the peptides and membranes. Peptide **1** was efficiently internalized into HeLa cells, whereas peptides **2** and **3** showed a much lower intracellular delivery.

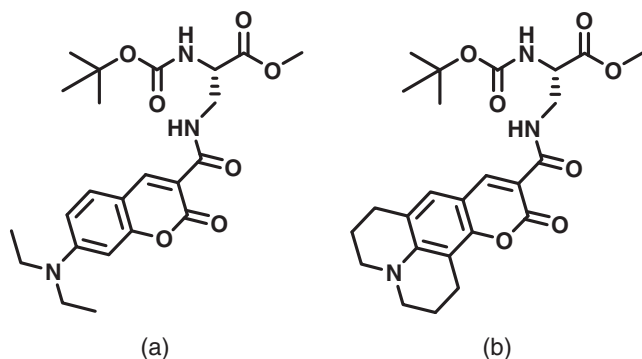
Peptide-based fluorescent biosensors^{1,2} have been developed for investigating the interactions between peptides and biological membranes,^{3–6} for detecting ions^{7–10} and studying protein functions^{11–16} in living cells, and for various biomedical applications.^{17–20} Fluorescent peptides are often imparted with fluorogenic properties to visualize biologically targeted substances or events in living organisms. One way to achieve this is to synthesize fluorogenic peptides with excitation donor and acceptor units or with a quenching unit having a fluorescent group. The fluorescence intensity of these peptides is enhanced through Förster resonance energy transfer or suppression of electron-transfer quenching induced by structural changes in the peptide in response to the detection of the targeted substances or biological events. Another approach involves using an environment-sensitive fluorophore that exhibits distinct fluorescence properties (e.g., fluorescence quantum yield, lifetime, and wavelength) when it binds with targeted substances or when a certain biological event occurs. This approach has been used to turn the fluorescence of labeled peptides on and off.^{1,2,5,21} This latter approach has the advantage that the labeled peptides are simple to synthesize and it is particularly useful for investigating peptide-membrane interactions in real-time.

Water-sensitive fluorophores that exhibit intense visible fluorescence in nonaqueous environments but whose fluorescence is remarkably quenched in aqueous media are especially useful for investigating protein functions in living cells and interactions between peptides and biological membranes. Typi-

cal water-sensitive fluorophores used in biological studies include 2-dimethylamino-6-propionyl-naphthalene,²² nitrobenzofurazan,²³ dimethylaminonaphthalenesulfonyl,²⁴ *N,N*-dimethylamino-1,8-naphthalimide,²⁵ and coumarin derivatives.²⁶ We recently synthesized a small fluorescent amino acid 3-[2-cyano-4-(dimethylamino)phenyl]alanine that is almost nonfluorescent in water but whose fluorescence intensity and lifetime are significantly enhanced when the molecule partitions to nonaqueous environments.²⁷ We have also developed a new fluorophore 8-methoxy-4-methyl-2*H*-benzo[*g*]-chromen-2-one that displays the opposite behavior: it is almost nonfluorescent in nonpolar aprotic media, but becomes highly emissive in polar protic media such as water.²⁸

To apply these environment-sensitive fluorophores to biological studies, it is essential to determine the photophysical mechanism of the environment-sensitive fluorescence. This study focuses on aminocoumarins. They are attractive fluorophores due to their relatively long-wavelength absorption and fluorescence spectra, high emission quantum yield, high photostability, and excellent environment-sensitive emission properties.^{26,29} Synthesis of fluorescent coumarin-bearing amino acids has been reported for biological imaging.³⁰ Aminocoumarin-labeled peptides with fluorogenic activity have also been synthesized for fluorescence imaging of proteins.³¹

In this study, we synthesized fluorescent amino acids bearing a fluorophore (7DEAC or C343) and evaluated their potential as fluorescence units for peptide-based fluorescent biosensors by examining their photophysical properties. The two



Scheme 1. Structures of (a) Boc-L-Dap(7DEAC)-OMe and (b) Boc-L-Dap(C343)-OMe.

fluorophores were incorporated into the side chain amino group of Dap (L-2,3-diaminopropionic acid) via amide bond. Furthermore, short fluorescent peptides H-Dap(7DEAC)-LLA-OMe (**1**), H-Dap(7DEAC)-KLA-OMe (**2**), and H-Dap(7DEAC)-ELA-OMe (**3**) labeled with environment-sensitive 7DEAC were synthesized to examine the interactions of the labeled peptides with lipid membranes and living cells. These tetrapeptides consist of three different dipeptide units containing fluorescent L-Dap(7DEAC) residue at N-terminal (Dap(7DEAC)-X; X = L (Leu), K (Lys), and E (Glu)). In addition, hydrophobic dipeptide ester moiety (LA-OMe) was incorporated to assist the entry of the labeled peptides into the lipid membrane since the LA sequence is frequently used in the model peptides of transmembrane helices^{32,33} and coiled-coil peptides.³¹ Peptides **1–3** possess distinct charge and hydrophobicity. They are thus expected to exhibit different affinities to biological membranes.

Results and Discussion

Photophysical Properties of Boc-L-Dap(7DEAC)-OMe and Boc-L-Dap(C343)-OMe. We synthesized protected nonnatural amino acids Boc-L-Dap(7DEAC)-OMe and Boc-L-Dap(C343)-OMe (Scheme 1) to evaluate their suitability as environment-sensitive fluorescent units of peptide-based fluorescent biosensors. Their photophysical properties were measured in various solvents that have different polarities and hydrogen-bonding abilities to determine their environment-sensitive properties. Figure 1 shows the absorption and fluorescence spectra of Boc-L-Dap(7DEAC)-OMe and Boc-L-Dap(C343)-OMe obtained in nonpolar solvent *n*-hexane, polar solvents acetonitrile (MeCN), and Tris-HCl/MeOH (9:1, v/v) at 20 °C. The absorption and fluorescence spectra of both compounds exhibit similar shapes and shift remarkably to the red when the solvent is changed from nonpolar *n*-hexane to polar MeCN and Tris-HCl/MeOH. In these solvents the absorption and fluorescence bands of Boc-L-Dap(C343)-OMe are shifted to wavelengths that are 15–20 nm longer than those of Boc-L-Dap(7DEAC)-OMe. The large red shifts in the absorption spectra observed when the solvent was changed from a nonpolar solvent to a polar solvent suggest that the dipole moment of the molecules is enhanced by the electronic transition to the S₁ state.

Table 1 lists the absorption and fluorescence maxima ($\lambda_{\max}^{\text{abs}}$ and $\lambda_{\max}^{\text{flu}}$) and the Stokes shift ($\Delta\bar{\nu}$) of Boc-L-Dap(7DEAC)-OMe and Boc-L-Dap(C343)-OMe together with the solvent

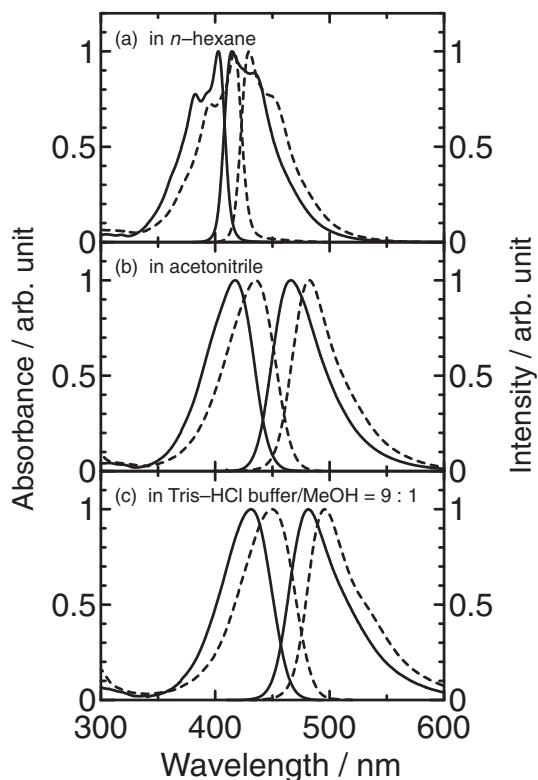


Figure 1. Absorption and fluorescence spectra of Boc-L-Dap(7DEAC)-OMe (solid line) and Boc-L-Dap(C343)-OMe (broken line) in (a) *n*-hexane, (b) MeCN, and (c) Tris-HCl buffer/MeOH (9:1 v/v) at 20 °C. λ_{exc} : (a) 370 and 380 nm, (b) 390 and 400 nm, and (c) 400 and 420 nm for Boc-L-Dap(7DEAC)-OMe and Boc-L-Dap(C343)-OMe, respectively.

properties, namely Taft's hydrogen-bonding ability (α), the dielectric constant (ϵ), and the orientation polarizability (Δf), which is given by:

$$\Delta f = f(\epsilon) - f(n^2) = \frac{\epsilon - 1}{2\epsilon + 1} - \frac{n^2 - 1}{2n^2 + 1} \quad (1)$$

where $f(\epsilon)$ and $f(n^2)$ are respectively the high and low frequency polarizabilities.³⁴ At high solvent polarities, the absorption and fluorescence spectra exhibit significant red shifts on changing the solvent from *n*-hexane to Tris-HCl/MeOH (9:1, v/v): 28 and 65 nm respectively for $\lambda_{\max}^{\text{abs}}$ and $\lambda_{\max}^{\text{flu}}$ of Boc-L-Dap(7DEAC)-OMe and 31 and 66 nm respectively for $\lambda_{\max}^{\text{abs}}$ and $\lambda_{\max}^{\text{flu}}$ of Boc-L-Dap(C343)-OMe. The protic solvents with hydrogen-donating ability increase the red shifts in both the absorption and fluorescence spectra; this is probably due to the hydrogen-bonding interaction with the carbonyl oxygen in the coumarin unit. These findings indicate that Boc-L-Dap(7DEAC)-OMe and Boc-L-Dap(C343)-OMe exhibit intramolecular charge transfer from the diethyl amino group to the carbonyl moieties in the first excited singlet (S₁) state. In fact, Lippert–Mataga plots suggest that the ground and S₁ states of Boc-L-Dap(7DEAC)-OMe and Boc-L-Dap(C343)-OMe have relatively large dipole moment differences ($\mu_e - \mu_g = 2.52$ and 2.43 D, respectively)³⁵ (see Figure S1 in Supporting Information). In protic solvents, hydrogen-bonding interactions

Table 1. Absorption Maximum ($\lambda_{\max}^{\text{abs}}$), Fluorescence Maximum ($\lambda_{\max}^{\text{flu}}$), and Stokes Shift ($\Delta\bar{\nu}$) of Boc-L-Dap(7DEAC)-OMe and Boc-L-Dap(C343)-OMe in Selected Solvents with Different Polarity and Proton-Donor Ability at 20 °C

Solvents	α^{a}	ϵ^{b}	Δf^{c}	Boc-L-Dap(7DEAC)-OMe			Boc-L-Dap(C343)-OMe		
				$\lambda_{\max}^{\text{abs}}/\text{nm}$	$\lambda_{\max}^{\text{flu}}/\text{nm}$	$\Delta\bar{\nu}/10^3 \text{ cm}^{-1}$	$\lambda_{\max}^{\text{abs}}/\text{nm}$	$\lambda_{\max}^{\text{flu}}/\text{nm}$	$\Delta\bar{\nu}/10^3 \text{ cm}^{-1}$
<i>n</i> -Hexane	0.00	1.89	0.000	403	415	0.752	418	430	0.657
Dibutyl ether	0.00	3.08	0.0957	408	433	1.42	423	448	1.35
Diethyl ether	0.00	4.27	0.165	408	438	1.76	423	453	1.63
Ethyl acetate	0.00	6.08	0.201	412	452	2.24	428	467	2.06
Butyl cyanide	—	20.0	0.269	417	462	2.40	435	478	2.12
Propyl cyanide	—	24.8	0.280	417	463	2.45	435	479	2.18
Ethyl cyanide	—	29.7	0.292	417	464	2.52	435	480	2.23
Acetonitrile	0.19	36.6	0.305	417	466	2.62	435	482	2.30
Ethanol	0.83	25.3	0.290	419	466	2.47	437	483	2.19
2,2,2-Trifluoroethanol	1.51	27.7	0.316	431	471	2.06	450	487	1.72
Methanol	0.93	33.0	0.309	420	470	2.59	439	485	2.19
Tris-HCl/MeOH (9:1, v/v)	1.05	75.4	0.320	431	480	2.49	449	496	2.15

a) Hydrogen-bond donor ability of solvent. b) Dielectric constant of solvent. c) Orientational polarizability of solvents.

Table 2. Fluorescence Quantum Yield (Φ_{f}), Fluorescence Lifetime (τ_{f}), Fluorescence Rate Constant (k_{f}) and Nonradiative Rate Constant (k_{nr}) of Boc-L-Dap(7DEAC)-OMe and Boc-L-Dap(C343)-OMe in Selected Solvents at 20 °C

Solvents	Δf^{a}	Boc-L-Dap(7DEAC)-OMe				Boc-L-Dap(C343)-OMe			
		$\Phi_{\text{f}}^{\text{b}}$	$\tau_{\text{f}}^{\text{b}}/\text{ns}$	$k_{\text{f}}/10^8 \text{ s}^{-1}$	$k_{\text{nr}}/10^8 \text{ s}^{-1}$	$\Phi_{\text{f}}^{\text{b}}$	$\tau_{\text{f}}^{\text{b}}/\text{ns}$	$k_{\text{f}}/10^8 \text{ s}^{-1}$	$k_{\text{nr}}/10^8 \text{ s}^{-1}$
<i>n</i> -Hexane	0.000	0.86	2.6	3.3	0.54	0.80	2.9	2.8	0.69
Dibutyl ether	0.0957	0.95	2.7	3.5	0.19	0.93	3.0	3.1	0.23
Diethyl ether	0.165	0.96	2.9	3.3	0.14	0.94	3.3	2.8	0.18
Ethyl acetate	0.201	0.76	2.5	3.0	0.96	0.97	3.4	2.9	0.088
Butyl cyanide	0.269	0.24	0.87	2.8	8.7	0.85	3.5	2.4	0.43
Propyl cyanide	0.280	0.16	0.55	2.9	15	0.95	3.6	2.6	0.14
Ethyl cyanide	0.292	0.10	0.36	2.8	25	0.90	3.7	2.4	0.27
Acetonitrile	0.305	0.065	0.23	2.8	41	0.94	3.8	2.5	0.16
Ethanol	0.290	0.085	0.27	3.1	34	0.93	3.7	2.5	0.19
2,2,2-Trifluoroethanol	0.316	0.037	0.15	2.5	64	0.95	4.3	2.2	0.12
Methanol	0.309	0.034	0.13	2.6	74	0.95	3.9	2.4	0.13
Tris-HCl/MeOH (9:1, v/v)	0.320	0.018	0.072	2.5	136	0.89	4.1	2.2	0.27

a) Orientational polarizability of solvents. b) Error is within 10%.

between proton-donating solvents and the carbonyl moieties of aminocoumarins are enhanced in the S_1 state that has charge-transfer character. This may further stabilize the excited state.

The fluorescence decay profiles were measured by exciting Boc-L-Dap(7DEAC)-OMe and Boc-L-Dap(C343)-OMe; they exhibited single exponential decays in all the solvents. Table 2 lists the fluorescence quantum yield (Φ_{f}) and the fluorescence lifetime (τ_{f}) along with the radiative (k_{f}) and nonradiative (k_{nr}) rate constants, which were calculated from Φ_{f} and τ_{f} using the following equations.

$$k_{\text{f}} = \Phi_{\text{f}}/\tau_{\text{f}}, \quad k_{\text{nr}} = (1 - \Phi_{\text{f}})/\tau_{\text{f}} \quad (2)$$

Table 2 shows that the fluorescence quantum yield and fluorescence lifetime of Boc-L-Dap(7DEAC)-OMe vary remarkably with the solvent properties: an increase in the solvent polarity significantly reduces Φ_{f} and τ_{f} due to an enhanced nonradiative rate. In particular, the most remarkable quenching is observed in strongly proton-donating solvents such as 2,2,2-trifluoroethanol and Tris-HCl/MeOH (9:1). The nonradiative rate constant of Boc-L-Dap(7DEAC)-OMe in Tris-HCl/MeOH (9:1) is of the order of 10^{10} s^{-1} , which suggests that

hydrogen-bonding interactions enhance the nonradiative rate. Ramakrishna and Ghosh³⁶ have reported similar photophysical properties for a similar coumarin derivative, 7-diethylamino-coumarin-3-carboxylic acid.

In contrast to the environment-sensitive relaxation properties of excited Boc-L-Dap(7DEAC)-OMe, the fluorescence quantum yield and lifetime of Boc-L-Dap(C343)-OMe are almost independent of the solvent parameters, as shown in Table 2. Specifically, the nonradiative transition rates are little affected by changes in the solvent polarity and the hydrogen-bonding ability, despite the remarkable shifts in the absorption and fluorescence spectra with changing the solvent polarity. Moreover, the fluorescence quantum yield is close to unity irrespective of the solvent properties. The most remarkable difference between the fluorophores in Boc-L-Dap(7DEAC)-OMe and Boc-L-Dap(C343)-OMe is that the internal rotational motion and out-of-bending vibrations of the amino group are structurally restricted in C343, unlike in 7DEAC. This clearly suggests that the structural changes in the diethylamino group on electronic excitation are responsible for the environment-sensitive photophysical character of Boc-L-Dap(7DEAC)-OMe.

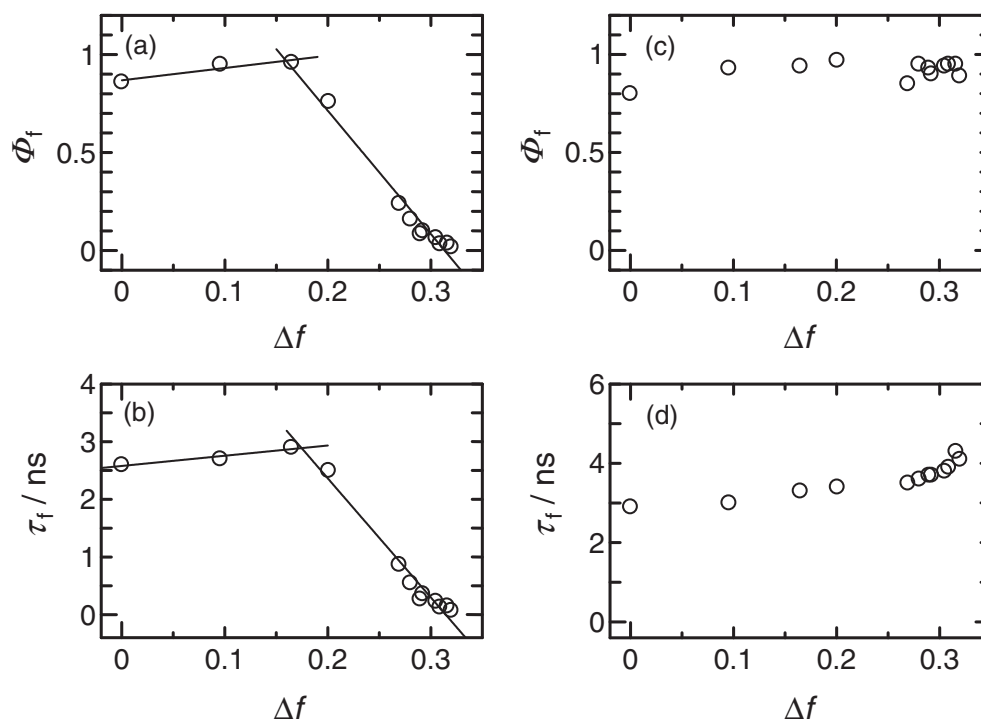
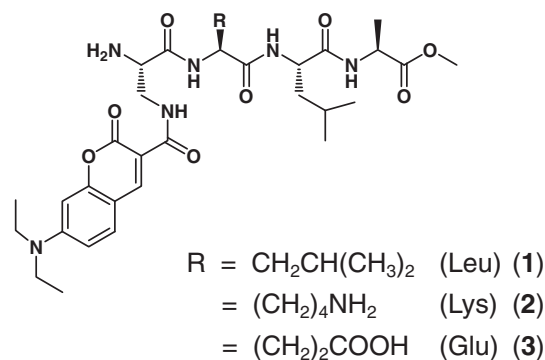


Figure 2. Plots of fluorescence quantum yield (Φ_f) and lifetime (τ_f) of Boc-L-Dap(7DEAC)-OMe ((a) and (b)) and Boc-L-Dap(C343)-OMe ((c) and (d)) against solvent parameter (Δf).

Figure 2 shows a plot of Φ_f and τ_f of Boc-L-Dap(7DEAC)-OMe and Boc-L-Dap(C343)-OMe as a function of the solvent polarity parameter (Δf). Interestingly, the plots for Boc-L-Dap(7DEAC)-OMe (Figures 2a and 2b) show that Φ_f and τ_f increase gradually with increasing solvent polarity, whereas in highly polar solvents with Δf larger than ca. 0.17, Φ_f and τ_f tend to decrease rapidly. In contrast, Φ_f and τ_f of Boc-L-Dap(C343)-OMe (Figures 2c and 2d) are almost constant in all the solvents used, although moderate increases in τ_f are observed in strongly polar solvents. The drastic changes in the solvent polarity dependences of Φ_f and τ_f , which were observed only in Boc-L-Dap(7DEAC)-OMe, suggest that a polarity-dependent nonradiative route opened in solvents with Δf larger than ca. 0.17 due to conformational changes in the diethylamino group in the excited state.^{26,36}

The distinct photophysical properties of Boc-L-Dap(7DEAC)-OMe and Boc-L-Dap(C343)-OMe suggest that 7DEAC can be used as a fluorophore for developing an environment-sensitive fluorescent probe that is water sensitive, while C343 is suitable for use as a biological labeling agent that does not respond to the surrounding environment.

Affinity of Coumarin-Labeled Peptides to Lipid Bilayer Membranes. We synthesized three 7DEAC-labeled peptides 1–3 (Scheme 2) to examine the interactions between the labeled peptides and lipid membranes through the environment-sensitive fluorescence character of 7DEAC. Coumarin-labeled compounds 1–3 are tetrapeptides, which have a residue with a distinct charge in the second position from the N-terminus. Peptide 1 has a neutral amino acid leucine, while peptides 2 and 3 respectively have a cationic lysine and anionic glutamic acid as the second residue. As mentioned in the previous section, 7DEAC has a very low fluorescence quantum



Scheme 2. Structures of coumarin-labeled peptides 1–3.

yield in aqueous media, whereas it is much higher in non-aqueous and less polar environments. Due to the environment-sensitive character of 7DEAC, fluorescence enhancement is expected to occur when the 7DEAC-labeled peptides interact with lipid bilayers. In addition, the fluorescence spectra will shift to shorter wavelengths when the peptides are partitioned into hydrophobic and less polar sites in lipid bilayer membranes from the highly polar aqueous phase.

To examine the affinity of coumarin-labeled peptides 1–3 with lipid bilayer membranes, we employed zwitterionic 1,2-dimyristoyl-*sn*-glycero-3-phosphocholine (DMPC) and anionic 1,2-dimyristoyl-*sn*-glycero-3-[phospho-*rac*-(1-glycerol)] (DMPG) membranes. Unilamellar vesicles composed of DMPC or DMPC/DMPG (1:1) membranes were prepared at 35 °C. The fluorescent peptide concentration was adjusted to be 1 μ M. Figure 3 shows the variation of the fluorescence spectra of 1–3 on adding DMPC (0.2–5.0 mM) and DMPC/DMPG (1:1) (0.02–1.0 mM) liposomes to a Tris-HCl buffer (pH 7.0) at

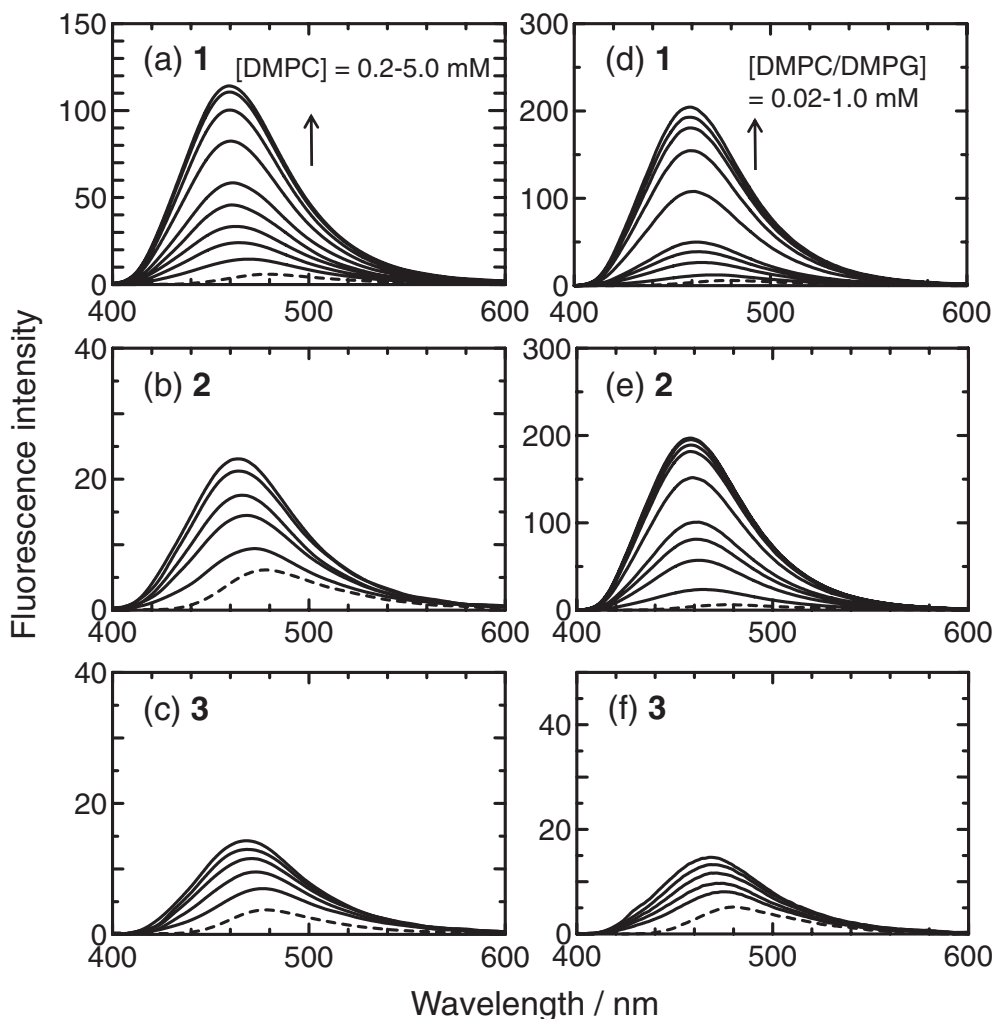


Figure 3. Fluorescence spectral changes of peptides (a) **1**, (b) **2**, and (c) **3** ($1\ \mu\text{M}$) on addition of 0.2–5.0 mM DMPC liposomes, and (d) **1**, (e) **2**, and (f) **3** ($1\ \mu\text{M}$) on addition of 0.02–1.0 mM DMPC/DMPG (1:1) liposomes in Tris-HCl buffer (pH 7.0) at 35 °C. The broken line represents the fluorescence spectra of **1–3** in Tris-HCl buffer (pH 7.0) without addition of liposomes (λ_{exc} : 380 nm).

35 °C. Figures 3a–3c show that the fluorescence intensity due to the 7DEAC moiety in the peptide increases significantly and the spectral peak shifts to the blue with increasing DMPC concentration, demonstrating that peptides **1–3** are partitioned inside the DMPC membrane. Similar changes in the fluorescence spectra of **1–3** are also observed for DMPC/DMPG (1:1) (0.02–1.0 mM) liposomes (Figures 3d–3f), although the degree of enhancement depends on the type of membrane.

To quantify the extent of the interaction of the peptides with the membrane model system, the partition coefficient (K_p) between the lipid and aqueous phases is defined as

$$K_p = \frac{n_L/V_L}{n_W/V_W} \quad (3)$$

where n_L and n_W are respectively the moles of peptide in lipid and water phases and V_L and V_W are respectively the volumes of lipid and water. From plots of the integrated fluorescence intensity I of the peptides against the concentration of DMPC or DMPC/DMPG (1:1) in Tris-HCl buffer (Figure 4), K_p between the lipid and aqueous phases was determined using:³⁷

$$I = \frac{I_w + K_p \gamma_L [L] I_L}{1 + K_p \gamma_L [L]} \quad (4)$$

where I_w and I_L are respectively the maximum fluorescence intensities obtained when all the fluorescent peptides are in the water and in the membrane and γ_L is the molar volume of the membrane ($0.67\ \text{L mol}^{-1}$)³⁸ and $[L]$ is the lipid concentration. Peptide **1** was partitioned into the DMPC and DMPC/DMPG (1:1) membranes with $K_p = 4.9 (\pm 0.5) \times 10^2$ and $4.2 (\pm 0.4) \times 10^3$, respectively. Cationic peptide **2** was more efficiently incorporated into the DMPC/DMPG membrane with $K_p = 1.4 (\pm 0.1) \times 10^4$, although it seems to have a much lower affinity to the DMPC membrane than to the DMPC/DMPG (1:1) membrane. These findings indicate that the negative charge of the DMPG membrane facilitates interactions between the membrane and peptide **2**, which has a positively charged lysine residue. Peptide **3**, which has a negative charge on the glutamic acid residue, was not partitioned efficiently into either membrane, probably due to repulsive interactions with DMPG. These results indicate that hydrophobic and electrostatic inter-

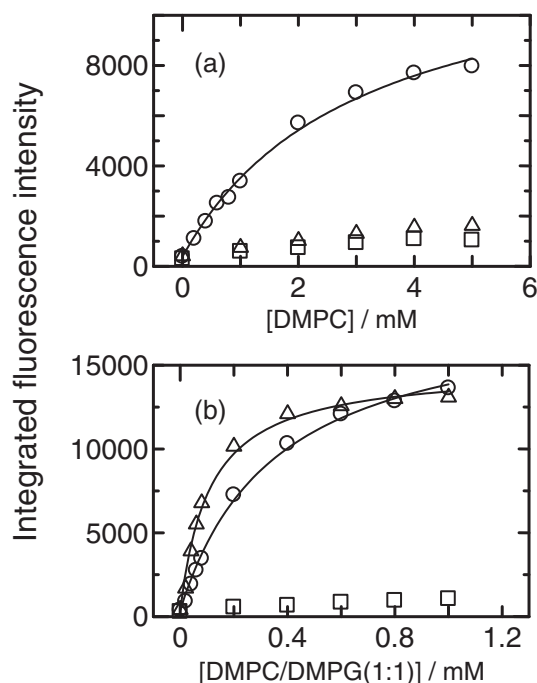


Figure 4. Fluorescence intensity changes of **1** (○), **2** (△), and **3** (□) (1 μM) vs. (a) DMPC and (b) DMPC/DMPG concentrations in Tris-HCl buffer (pH 7.0) at 35 °C.

actions play an important role in determining the affinity of short peptides to lipid bilayer membranes.³⁹

Fluorescence Decay Characteristics of Coumarin-Labeled Peptides in Lipid Bilayer Membranes. Measuring the fluorescence decay characteristics is a powerful approach for directly monitoring the environment and dynamics around a fluorescent peptide, which reflects interactions with lipid bilayer membranes. Figures 5a–5c show the fluorescence decay profiles of peptide **1** (1 μM) in Tris-HCl buffer and in the presence of DMPC (1 mM) and DMPC/DMPG (1:1; 1 mM) liposomes in Tris-HCl buffer at 35 °C, respectively. The fluorescence decay curves were deconvoluted with the instrument response function and analyzed as a sum of exponential terms:

$$F(t) = \sum_i A_i \exp(-t/\tau_i) \quad (5)$$

where $F(t)$ is the fluorescence intensity at time t , and τ_i and A_i are respectively the lifetime and the pre-exponential factor of the i th component. The average lifetime was calculated from τ_i and A_i using

$$\langle \tau \rangle = \frac{\sum_{i=1}^n A_i \tau_i^2}{\sum_{i=1}^n A_i \tau_i} \quad (6)$$

The fluorescence decay profile of peptide **1** in Tris-HCl buffer (Figure 5a) could be analyzed by a single exponential with a lifetime of 62 ps, while much slower decay components were observed in the presence of DMPC (1 mM) (Figure 5b) and the decay curve was best fitted using three decay components with lifetimes of 65 ps ($A_1 = 0.12$), 805 ps ($A_2 = 0.42$), and 1.92 ns ($A_3 = 0.46$). The shortest lifetime (65 ps) component is very

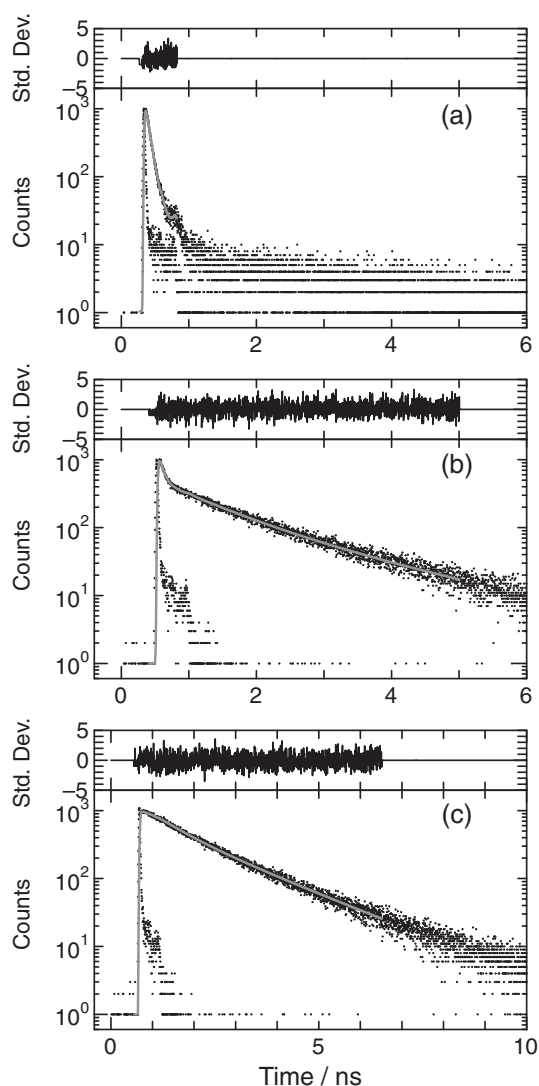


Figure 5. Fluorescence decay profiles of **1** (1 μM) in (a) Tris-HCl buffer (pH 7.0) and in Tris-HCl buffer under the presence of (b) DMPC (1 mM) and (c) DMPC/DMPG (1:1; 1 mM) at 35 °C. λ_{exc} : 266 nm and λ_{mon} : (a) 480, (b) 461, and (c) 458 nm.

close to the lifetime observed in buffer solutions, which suggests that this component originates from peptide **1** molecules in the water phase (i.e., on the outside of the liposomes). The proportion (12%) of the shortest lifetime component is much lower than that (88%) of the longer lifetime components, which are not observed for peptides in buffer solutions. These results clearly show that most of peptide **1** is incorporated into the liposome membrane, which is consistent with the relatively large K_p value ($4.9 (\pm 0.5) \times 10^2$) of **1** in DMPC membranes. The observation of two long-lifetime components (805 ps and 1.92 ns) suggests that peptide **1** is localized in at least two distinct sites with different polarities in DMPC liposome membranes. It is conceivable from Table 2 that peptide **1** molecules, which give the longest lifetime (1.92 ns) component with the pre-exponential factor of 0.46, are localized in a site with its polarity between ethyl acetate and *n*-butyl cyanide in liposome membranes. In the same way, peptide **1** molecules, which give

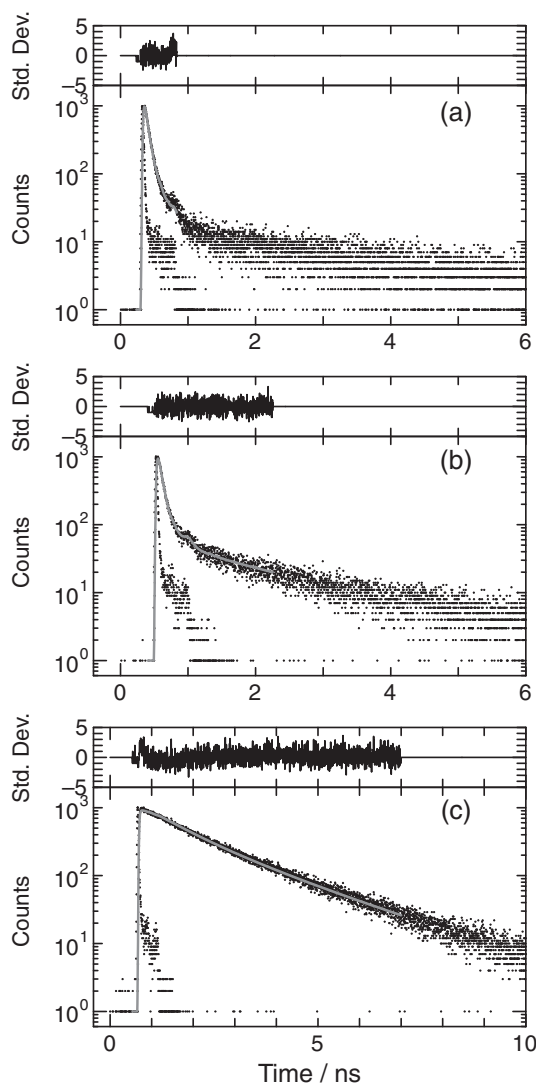


Figure 6. Fluorescence decay profiles of **2** (1 μ M) in (a) Tris-HCl buffer (pH 7.0) and in Tris-HCl buffer under the presence of (b) DMPC (1 mM) and (c) DMPC/DMPG (1:1; 1 mM) at 35 $^{\circ}$ C. λ_{exc} : 266 nm and λ_{mon} : (a) 476, (b) 472, and (c) 457 nm.

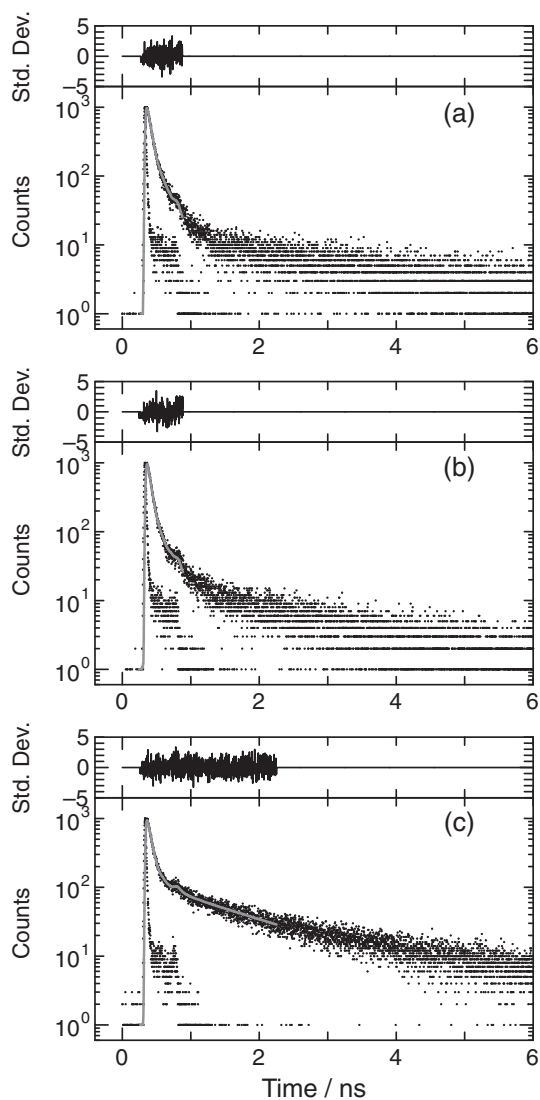


Figure 7. Fluorescence decay profiles of **3** (1 μ M) in (a) Tris-HCl buffer (pH 7.0) and in Tris-HCl buffer under the presence of (b) DMPC (1 mM) and, (c) DMPC/DMPG (1:1; 1 mM) at 35 $^{\circ}$ C. λ_{exc} : 266 nm and λ_{mon} : (a) 480, (b) 476, and (c) 468 nm.

the second lifetime (805 ps) component with the pre-exponential factor of 0.42, are considered to be localized in a site with its polarity between butyl cyanide and propyl cyanide, i.e., a more polar site with its location close to the head group of the liposome membranes. In the presence of DMPC/DMPG (1:1) liposomes, the shortest lifetime component almost disappeared and the fluorescence profile could be analyzed in terms of two exponential decays with lifetimes of 638 ps ($A_1 = 0.22$) and 1.74 ns ($A_2 = 0.78$). This indicates that almost all the peptide molecules are bound to DMPC/DMPG (1:1) membranes and hence the higher affinity to DMPC/DMPG (1:1) membranes is probably due to electrostatic interactions between the protonated N-terminus of the peptide and the anionic DMPG lipid in DMPC/DMPG (1:1) membranes.

Figures 6 and 7 respectively show the fluorescence decay profiles of peptides **2** and **3** in Tris-HCl buffer and in lipid membranes. Table 3 lists the results of fluorescence decay

analysis together with the result of **1**. The fluorescence decay curves of **2** and **3** in Tris-HCl buffer were best analyzed by two exponentials with lifetimes of 50–60 and 150–190 ps (Table 3). Although the origin of the two exponential decay components in Tris-HCl buffer is not obvious, one possible explanation is given in terms of different conformers that can be involved in labeled peptides in water.²⁷ In the presence of DMPC, peptide **2** has a much slower decay component with a lifetime of 1.63 ns ($A_2 = 0.45$), in addition to the fast decay component with a lifetime of 0.063 ns ($A_1 = 0.55$). Here, the magnitude of the pre-exponential factor is not quantitatively related to partitioning of the peptides between the membrane and the aqueous phase due to the fluorescence spectral shift accompanying partitioning of the peptides into the less polar membrane. However, the above result suggests that nearly half of peptide **2** is bound to the DMPC membrane. In the presence of DMPC/DMPG (1:1) membranes, the component with lifetimes of 50–

Table 3. Fluorescence Lifetimes of **1–3** (1 μ M) under the Presence of DMPC (1 mM) and DMPC/DMPG (1:1; 1 mM) Membranes in Tris-HCl Buffer (pH 7.0) at 35 $^{\circ}$ C

Compounds	Lipid	$\lambda_{\text{mon}}/\text{nm}$	τ/ns	A_1	τ_2/ns	A_2	τ_3/ns	A_3	$\langle\tau\rangle/\text{ns}$	χ^2
1	No Lipid	480	0.062	1.00					0.062	1.03
	DMPC	461	0.065	0.12	0.805	0.42	1.92	0.46	1.23	1.05
	DMPC/DMPG	458	0.638	0.22	1.74	0.78			1.50	1.02
2	No Lipid	476	0.052	0.76	0.155	0.24			0.077	1.13
	DMPC	472	0.063	0.55	1.63	0.45			0.77	0.99
	DMPC/DMPG	457	0.88	0.34	2.07	0.66			1.67	1.13
3	No Lipid	480	0.056	0.70	0.182	0.30			0.094	1.20
	DMPC	476	0.053	0.75	0.244	0.25			0.102	1.02
	DMPC/DMPG	468	0.062	0.39	1.37	0.61			0.86	1.01

60 ps almost disappeared and the proportion of the long lifetime (2.07 ns) component increased in peptide **2**, which is in agreement with the large K_p value ($1.4 (\pm 0.1) \times 10^4$) of **2** in DMPC/DMPG membranes.

In contrast to peptide **2**, peptide **3** exhibits similar two-component decays in Tris-HCl buffer and in the same buffer containing DMPC liposomes. This shows that anionic peptide **3** has a very low affinity to the zwitterionic DMPC membrane. The decay profile of peptide **3** in the presence of DMPC/DMPG (1:1) membranes in Tris-HCl buffer was best fitted by two exponentials with lifetimes of 62 ps ($A_1 = 0.39$) and 1.37 ns ($A_2 = 0.61$). The lifetime of the faster decay component is close to that in Tris-HCl buffer. These findings show that peptide **3** has a much lower affinity to DMPC/DMPG (1:1) membranes than peptides **1** and **2**. The electrostatic repulsion between the anionic carboxy group of **3** and the negatively charged DMPG lipid in DMPC/DMPG (1:1) membranes is related to the lower affinity of **3** to DMPC/DMPG (1:1) membranes.

Hydrophobicity of the LA sequence in **1–3** will promote the incorporation of the labeled peptides into the hydrophobic region of lipid bilayer membranes, resulting in the appearance of the long lifetime components. On the other hand, the protonated amino group of the peptides will facilitate the electrostatic and/or hydrogen-bonding interactions of the peptides with the anionic head group of lipid membranes. The latter ionic interactions might be related to the second lifetime (805 ps) component observed for **1** and **2** in DMPC and/or DMPC/DMPG membranes, because partial water penetration occurs in the membrane interfacial region. In the case of the zwitterionic peptide **3**, however, such ionic interactions would be suppressed by the electrostatic repulsion due to the anionic carboxy group.

Affinity of Peptides 1–3 to Living Cells. We then investigated the interactions between peptides **1–3** and living cells (HeLa cells). Figures 8a–8c show emission images of HeLa cells that were loaded with peptides **1–3** (10 μ M). Peptide **1** gives a much brighter image than peptides **2** and **3**, showing that peptide **1** has a much higher cellular uptake efficiency than peptides **2** and **3**. The logarithm of the water–octanol partition coefficient ($\log P_{o/w}$) of a substance loaded into the cell medium is known to be correlated with the ability of the substance to penetrate the plasma membrane of living cells^{40,41} and it is used as a measure of molecular hydrophobicity. The $\log P_{o/w}$ values of our peptides **1–3** were obtained as 1.735,

–0.66, and 0.207, respectively. Goodwin et al. investigated the relationship between the transcellular permeability coefficients and $\log P_{o/w}$ by using a series of dipeptides⁴⁰ and found that the cellular permeability increases with increasing $\log P_{o/w}$, at least between $\log P_{o/w} = 0$ and 2. This is consistent with our results, namely that **1** ($\log P_{o/w} = 1.735$) has a much higher cellular uptake efficiency than **2** ($\log P_{o/w} = -0.66$) and **3** ($\log P_{o/w} = 0.207$).

We then verified the intracellular localization of peptide **1** in living cells by performing a morphologic examination using HeLa cells. Cellular localization of peptide **1** seemed to be limited to the cytoplasm and not to the nucleus (Figures 8d–8f). We examined color merging using the red lysosome-specific probe LysoTracker, and observed purple between peptide **1** and LysoTracker (Figure 8f). These observations suggest that peptide **1** exhibits selective lysosome localization in the cytoplasm.

Conclusion

The protected nonnatural amino acids Boc–L–Dap(7DEAC)–OMe and Boc–L–Dap(C343)–OMe were synthesized and their photophysical properties were examined in a series of solvents that have different polarities and hydrogen-bonding abilities. The fluorescence quantum yield and lifetime of Boc–L–Dap(7DEAC)–OMe decreased significantly from nonpolar *n*-hexane ($\Phi_f = 0.86$, $\tau_f = 2.6$ ns) to polar Tris-HCl/MeOH (9:1 v/v) mixed solvent ($\Phi_f = 0.018$, $\tau_f = 0.072$ ns), whereas those of Boc–L–Dap(C343)–OMe were almost independent of the solvent parameters. Short peptides H–Dap(7DEAC)–LLA–OMe (**1**), H–Dap(7DEAC)–KLA–OMe (**2**), and H–Dap(7DEAC)–ELA–OMe (**3**) labeled with environment-sensitive 7DEAC were synthesized to explore the application of 7DEAC to probe biological interactions. The fluorescence intensity of 7DEAC-labeled peptides **1–3** significantly increased upon binding to DMPC and DMPC/DMPG (1:1) liposomes in Tris-HCl buffer, showing that the affinity of **1–3** to these membranes depends on hydrophobic and electrostatic interactions. Furthermore, the fluorescence decay profiles of peptides **1–3** varied with affinities of the peptides to lipid membranes. These results indicate that the environment-sensitive fluorophore 7DEAC is useful for labeling peptides or proteins to monitor biological interactions.

Experimental

General. Absorption and emission spectra were respectively measured using a UV–vis spectrophotometer (Jasco,

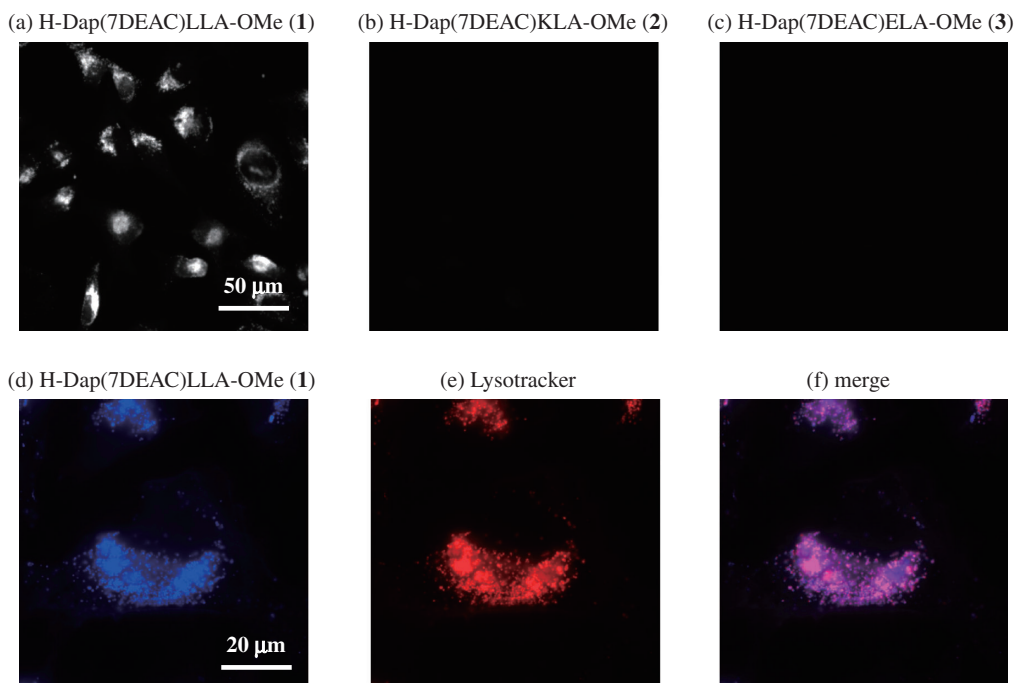


Figure 8. Upper: Luminescence images of HeLa cells treated with (a) **1**, (b) **2**, and (c) **3**. Lower: Subcellular localization of the peptide **1** in HeLa cells. Peptide **1** was added to the medium at a final concentration of 10 μM . Lysotracker (100 nM), which selectively stains lysosome, was used as an organelle marker.

Ubest-V550) and a spectrofluorometer (Hitachi, F-4010). The emission spectrum was corrected for spectral sensitivity. Picosecond fluorescence lifetime measurements were performed using a femtosecond laser system that was based on a mode-locked Ti:sapphire laser (Spectra-Physics, Tsunami; center wavelength: 800 nm; pulse width: ca. 70 fs; repetition rate: 82 MHz) pumped by a CW green laser (Spectra-Physics, Millennia V; 532 nm, 4.5 W).⁴² The repetition frequency was reduced to 4 MHz by using a pulse picker (Spectra-Physics, 3980) and the third harmonic (266 nm; FWHM: ca. 250 fs) was used as the excitation source. The monitoring system consisted of a microchannel plate photomultiplier tube (MCP-PMT; Hamamatsu, R3809U-51) that was cooled to $-20\text{ }^{\circ}\text{C}$ and a single-photon counting module (Becker and Hickl, SPC-530). The fluorescence photon signal detected by the MCP-PMT and the photon signal of the second harmonic (400 nm) of the Ti:sapphire laser were used for the start and stop pulses of a time-to-amplitude converter in this system. The instrument response function had a half width of about 25 ps. The fluorescence time profiles were analyzed by deconvoluting with the instrument response function.

Fluorescence quantum yields of all the compounds in de-aerated solution were measured using an absolute photoluminescence quantum yield system (Hamamatsu, C9920-02)⁴³ that consisted of a Xe arc lamp, a monochromator, an integrating sphere, a multichannel detector, and a personal computer.

Cellular Experiments. HeLa cells were purchased from American Type Culture Collection and were cultured in Dulbecco's Modified Eagle Medium supplemented with 10% fetal bovine serum, penicillin (50 units/mL), streptomycin (50 mg mL⁻¹) for 24 h at 37 $^{\circ}\text{C}$ in a 5% CO₂ atmosphere. Peptides **1–3** were added to the medium at a final concentration of

10 μM and the cells were incubated for 2 h. The medium was then removed and the cell layer was washed with phosphate-buffered saline. Luminescence microscopy images of HeLa cells treated with peptides **1–3** were obtained using an inverted microscope (Olympus, IX71) equipped with a $\times 40$ objective lens or a $\times 100$ oil-immersion objective lens and an electron multiplying CCD camera (Evolve 512, Photometrics) driven by MetaVue software. Samples were excited using a 100 W mercury lamp and imaged using custom filter settings (blue channel: excitation band path = 400–410 nm, emission band path = 460–510 nm; red channel: excitation band path = 545–580 nm, emission cut > 610 nm).

Materials. Solvents were of spectrograde quality if available and were used without further purification except propyl cyanide and ethyl cyanide which were purified by column chromatography (activated carbon and alumina). Deionized water was purified by using a Millipore (MILLI-Q-Labo).

Supporting Information

Synthesis of Boc-L-Dap(7DEAC)-OMe, Boc-L-Dap-(C343)-OMe, H-Dap(7DEAC)-LLA-OMe (**1**), H-Dap(7DEAC)-KLA-OMe (**2**), and H-Dap(7DEAC)-ELA-OMe (**3**). Lippert–Mataga plot. This material is available free of charge on the Web at <http://www.csj.jp/journals/bcsj/>.

References

- 1 E. Pazos, O. Vázquez, J. L. Mascareñas, M. E. Vázquez, *Chem. Soc. Rev.* **2009**, *38*, 3348.
- 2 A. R. Katritzky, T. Narindoshvili, *Org. Biomol. Chem.* **2009**, *7*, 627.
- 3 Z. Ningsih, M. A. Hossain, J. D. Wade, A. H. A. Clayton, M. L. Gee, *Langmuir* **2012**, *28*, 2217.

- 4 A. A. Strömstedt, L. Ringstad, A. Schmidtchen, M. Malmsten, *Curr. Opin. Colloid Interface Sci.* **2010**, *15*, 467.
- 5 A. P. Demchenko, Y. Mély, G. Duportail, A. S. Klymchenko, *Biophys. J.* **2009**, *96*, 3461.
- 6 L. You, G. W. Gokel, *Chem.—Eur. J.* **2008**, *14*, 5861.
- 7 Y. Li, L. Li, X. Pu, G. Ma, E. Wang, J. Kong, Z. Liu, Y. Liu, *Bioorg. Med. Chem. Lett.* **2012**, *22*, 4014.
- 8 B. P. Joshi, J. Park, W. I. Lee, K.-H. Lee, *Talanta* **2009**, *78*, 903.
- 9 J. C. Saucedo, R. M. Duke, M. Nitz, *ChemBioChem* **2007**, *8*, 391.
- 10 G. K. Walkup, B. Imperiali, *J. Am. Chem. Soc.* **1996**, *118*, 3053.
- 11 J. A. González-Vera, *Chem. Soc. Rev.* **2012**, *41*, 1652.
- 12 D. Sethi, C.-P. Chen, R.-Y. Jing, M. L. Thakur, E. Wickstrom, *Bioconjugate Chem.* **2012**, *23*, 158.
- 13 H.-W. Rhee, S. H. Lee, I.-S. Shin, S. J. Choi, H. H. Park, K. Han, T. H. Park, J.-I. Hong, *Angew. Chem., Int. Ed.* **2010**, *49*, 4919.
- 14 R. S. Agnes, F. Jernigan, J. R. Shell, V. Sharma, D. S. Lawrence, *J. Am. Chem. Soc.* **2010**, *132*, 6075.
- 15 K. Kikuchi, S. Hashimoto, S. Mizukami, T. Nagano, *Org. Lett.* **2009**, *11*, 2732.
- 16 A. Cobos-Correa, J. B. Trojanek, S. Diemer, M. A. Mall, C. Schultz, *Nat. Chem. Biol.* **2009**, *5*, 628.
- 17 M. H. Lee, J. Y. Kim, J. H. Han, S. Bhuniya, J. L. Sessler, C. Kang, J. S. Kim, *J. Am. Chem. Soc.* **2012**, *134*, 12668.
- 18 M. A. Whitney, J. L. Crisp, L. T. Nguyen, B. Friedman, L. A. Gross, P. Steinbach, R. Y. Tsien, Q. T. Nguyen, *Nat. Biotechnol.* **2011**, *29*, 352.
- 19 H. Luo, J. Yang, H. Jin, C. Huang, J. Fu, F. Yang, H. Gong, S. Zeng, Q. Luo, Z. Zhang, *FASEB J.* **2011**, *25*, 1865.
- 20 F. Crawford, B. Stadinski, N. Jin, A. Michels, M. Nakayama, P. Pratt, P. Marrack, G. Eisenbarth, J. W. Kappler, *Proc. Natl. Acad. Sci. U.S.A.* **2011**, *108*, 16729.
- 21 a) M. Taki, T. Hohsaka, H. Murakami, K. Taira, M. Sisido, *FEBS Lett.* **2001**, *507*, 35. b) M. E. Vázquez, D. M. Rothman, B. Imperiali, *Org. Biomol. Chem.* **2004**, *2*, 1965. c) M. E. Vázquez, J. B. Blanco, B. Imperiali, *J. Am. Chem. Soc.* **2005**, *127*, 1300.
- 22 G. Weber, F. J. Farris, *Biochemistry* **1979**, *18*, 3075.
- 23 a) P. B. Ghosh, M. W. Whitehouse, *Biochem. J.* **1968**, *108*, 155. b) S. Fery-Forgues, J.-P. Fayet, A. Lopez, *J. Photochem. Photobiol., A* **1993**, *70*, 229. c) H. Raghuraman, A. Chattopadhyay, *Biophys. J.* **2007**, *92*, 1271. d) S. Uchiyama, K. Kimura, C. Gota, K. Okabe, K. Kawamoto, N. Inada, T. Yoshihara, S. Tobita, *Chem.—Eur. J.* **2012**, *18*, 9552.
- 24 Y.-H. Li, L.-M. Chan, L. Tyer, R. T. Moody, C. M. Himel, D. M. Hercules, *J. Am. Chem. Soc.* **1975**, *97*, 3118.
- 25 G. Loving, B. Imperiali, *J. Am. Chem. Soc.* **2008**, *130*, 13630.
- 26 a) S. Nad, M. Kumbhakar, H. Pal, *J. Phys. Chem. A* **2003**, *107*, 4808. b) A. K. Satpati, M. Kumbhakar, S. Nath, H. Pal, *Photochem. Photobiol.* **2009**, *85*, 119.
- 27 a) J. Oshima, H. Tsujimoto, T. Yoshihara, K. Yamada, R. Katakai, S. Tobita, *Chem. Lett.* **2006**, *35*, 620. b) J. Oshima, S. Shiobara, H. Naoumi, S. Kaneko, T. Yoshihara, A. K. Mishra, S. Tobita, *J. Phys. Chem. A* **2006**, *110*, 4629.
- 28 a) S. Uchiyama, K. Takehira, T. Yoshihara, S. Tobita, T. Ohwada, *Org. Lett.* **2006**, *8*, 5869. b) A. Kobayashi, K. Takehira, T. Yoshihara, S. Uchiyama, S. Tobita, *Photochem. Photobiol. Sci.* **2012**, *11*, 1368.
- 29 E. H. El-Mossalamy, A. Y. Obaid, S. A. El-Daly, *Opt. Laser Technol.* **2011**, *43*, 1078.
- 30 a) M.-P. Brun, L. Bischoff, C. Garbay, *Angew. Chem., Int. Ed.* **2004**, *43*, 3432. b) T. Berthelot, G. Lain, L. Latxague, G. Déleris, *J. Fluoresc.* **2004**, *14*, 671. c) G. Sui, P. Kele, J. Orbulescu, Q. Huo, R. M. Leblanc, *Letts. Pept. Sci.* **2001**, *8*, 47.
- 31 H. Tsutsumi, S. Abe, T. Mino, W. Nomura, H. Tamamura, *ChemBioChem* **2011**, *12*, 691.
- 32 S. S. Krishnakumar, E. London, *J. Mol. Biol.* **2007**, *374*, 671.
- 33 a) Y. Yano, K. Matsuzaki, *Biochemistry* **2006**, *45*, 3370. b) Y. Yano, N. Shimai, K. Matsuzaki, *J. Phys. Chem. B* **2010**, *114*, 1925.
- 34 B. Valeur, *Molecular Fluorescence: Principles and Applications*, Wiley-VCH, Weinheim, **2001**. doi:10.1002/3527600248.
- 35 a) N. Mataga, Y. Kaifu, M. Koizumi, *Bull. Chem. Soc. Jpn.* **1955**, *28*, 690; N. Mataga, Y. Kaifu, M. Koizumi, *Bull. Chem. Soc. Jpn.* **1956**, *29*, 465. b) E. Lippert, *Z. Naturforsch., A* **1955**, *10*, 541; E. Lippert, *Z. Elektrochem.* **1957**, *61*, 962.
- 36 G. Ramakrishna, H. N. Ghosh, *J. Phys. Chem. A* **2002**, *106*, 2545.
- 37 N. C. Santos, M. Prieto, M. A. R. B. Castanho, *Biochim. Biophys. Acta, Biomembr.* **2003**, *1612*, 123.
- 38 D. Marsh, *Handbook of Lipid Bilayers*, CRC Press, Boca Raton, FL, **1990**, pp. 188–190.
- 39 G. Denisov, S. Wanaski, P. Luan, M. Glaser, S. McLaughlin, *Biophys. J.* **1998**, *74*, 731.
- 40 J. T. Goodwin, R. A. Conradi, N. F. H. Ho, P. S. Burton, *J. Med. Chem.* **2001**, *44*, 3721.
- 41 R. W. Horobin, J. C. Stockert, F. Rashid-Doubell, *Histochem. Cell Biol.* **2006**, *126*, 165.
- 42 S. Kaneko, S. Yotoriyama, H. Koda, S. Tobita, *J. Phys. Chem. A* **2009**, *113*, 3021.
- 43 a) K. Suzuki, A. Kobayashi, S. Kaneko, K. Takehira, T. Yoshihara, H. Ishida, Y. Shiina, S. Oishi, S. Tobita, *Phys. Chem. Chem. Phys.* **2009**, *11*, 9850. b) H. Ishida, S. Tobita, Y. Hasegawa, R. Katoh, K. Nozaki, *Coord. Chem. Rev.* **2010**, *254*, 2449.